B. TECH. PROJECT REPORT

On

PERFORMANCE ANALYSIS OF ADAPTIVE-COMBINING-BASED HYBRID FSO/RF SATELLITE COMMUNICATION

BY

Suyash Shah

DISCIPLINE OF ELECTRICAL ENGINEERING

INDIAN INSTITUTE OF TECHNOLOGY INDORE

December 2019

PERFORMANCE ANALYSIS OF ADAPTIVE-COMBINING-BASED HYBRID FSO/RF SATELLITE COMMUNICATION

A PROJECT REPORT

Submitted in partial fulfillment of the requirements for the award of the degrees

of
BACHELOR OF TECHNOLOGY
in

Electrical ENGINEERING

Submitted by:
Suyash Shah

Guided by:
Dr Swaminathan R.

INDIAN INSTITUTE OF TECHNOLOGY INDORE
DECEMBER 2019

CANDIDATE'S DECLARATION

We hereby declare that the project entitled **"Performance analysis of adaptive combining-based hybrid FSO/RF satellite communication"** submitted in partial fulfillment for the award of the degree of Bachelor of Technology in 'Electrical Engineering' completed under the supervision of **Dr. Swaminathan R., Assistant Professor,** Discipline of Electrical Engineering, IIT Indore is an authentic work.

Further, I declare that I have not submitted this work for the award of any other degree elsewhere.

Signature and name of the student with date

CERTIFICATE by BTP Guide

It is certified that the above statement made by the students is correct to the best of my knowledge.

Signature of BTP Guide with dates and their designation

<u>Preface</u>

This report on “Performance analysis of adaptive combining-based hybrid FSO/RF satellite communication " is prepared under the guidance of Dr. Swaminathan R..

In this thesis I have extensively discussed the performance analysis of single hop and dual hop hybrid free space optics/ radio frequency satellite communication system. I have also included the asymptotic analysis of the outage probability and average symbol error rate. Numerical results are also discussed in this thesis and an elaborate discussions of the results are presented with graphs and figures.

Suyash Shah
B.Tech. IV Year
Discipline of Electrical Engineering
IIT Indore

Acknowledgements

I wish to thank Dr. Swaminathan R. for his kind support and valuable guidance. It is his help and support due to which I could complete the design, analysis and technical report. Without his support this report would not have been possible.

Suyash Shah
B.Tech. IV Year
Discipline of Electrical Engineering
IIT Indore

Abstract

The widespread use of radio frequency (RF) system has made the electromagnetic spectrum (EMS) a scarce resource. Licensing and high pricing of the sub-bands are a common feat. Moreover, the EMS of the RF wave is fundamentally limited in its data-carrying capacity. So, there is a need to explore and develop communication technology which can cater to the need of modern developments providing sufficient bandwidth to operate and higher data rate for better inter-connectivity. Free space optics (FSO) is one such system which can give us access to the otherwise untouched EMS and can support a high data rate. However, FSO link is susceptible to atmospheric turbulence and pointing error which make it necessary to back it up by a reliable RF link. These systems are called hybrid FSO/RF systems. Hybrid FSO/RF system uses the complementary nature of FSO and RF link to provide a reliable communication link.

In this thesis, we have analysed the outage probability and average symbol error rate (SER) of the adaptive combining based switching scheme for space-air-ground integrated hybrid FSO/RF system considering both up-link and down-link scenarios with and without high altitude pseudo satellite (HAPS). Adaptive combining based switching (ACBS) uses FSO link as a primary link and RF link only as a backup link. In ACBS, data is continuously transmitted over the FSO link while the RF link is only active when the quality of RF link deteriorates. The outage and average SER analysis have been carried out assuming Ricean distribution for RF channel modelling, and Gamma-Gamma distribution for FSO channel modelling. The performance of ACBS is compared with hard switching and single link FSO system. Further, asymptotic analysis has been carried out to obtain the diversity gain of the ACBS base hybrid FSO/RF system. From the numerical results, it has been observed that the backup RF links and HAPS with ACBS help in improving the performance of FSO communication.

Contents

List of Figures

List of Tables

Chapter 1

Introduction

The ever-growing advancements in technology have made systems inter-dependent. The data generated per second today is enormous. The interdependence of the systems to analyse and to operate on the data generated has made it a requirement for communication systems to be reliable and to work at a higher data rate than the earlier.

High altitude pseudo satellite (HAPS) are aircraft stationed in the lower stratosphere typically at the height of around 17 to 25 km. These act as a pseudo satellite to provide services which are generally offered by satellite. Unmanned areal vehicle (UAV), balloons and airships can be used as HAPS. Further, HAPS find various potential applications in disaster monitoring, agricultural observation, atmospheric observation, weather monitoring and communication relay [1]. HAPS has multiple advantages over satellite. They can provide better coverage of smaller regions as compared to satellites. Moreover, they are easier and cheaper to deploy and maintain. HAPS, when used as a relay node [2], can improve the performance of communication between ground station (GS) and satellite.

The systems used today for wireless communication have become synonymous to radio-frequency (RF) technology because of the wide-scale research, development and deployment of the RF systems. However, this large scale use of the RF systems has made the electromagnetic spectrum (EMS) a scarce resource due to which most sub-bands are exclusively licensed and costly. Moreover, the EMS of the RF wave is fundamentally limited in its capacity to carry the data only up to a specific rate. To cater to the needs of the advancements, we need to explore other viable communication systems which can operate in higher EMS, thus having a higher data rate and opening the untouched EMS to operate.

These have fostered the development of various communication technologies, one of which is optical wireless communication (OWC). OWC refers to the transmission of data in unguided propagation medium through the use of optical carriers in visible IR and UV bands [3]. The outdoor OWC is generally referred to as free-space optics (FSO). It has the capability to tap in the otherwise untouched higher EMS providing us with higher data rate up to terabits per second which is a significant increase as compared to the RF link which can offer data rate only up to a few hundred megabits per seconds. FSO uses very narrow beams of laser for transmission. This spacial confinement of the FSO beam provides immunity towards electromagnetic interference, a high reuse factor and inherent security [3]. The FSO link provides a high data transfer rate for short-range transmission because of its susceptibility to the different atmospheric condition such as rain, fog and atmospheric turbulence-induced fading, which affects its reliability over the long-range transmission. Due to which it becomes necessary to back it by a reliable RF link.

The application of the FSO link in satellite communication (SATCOM) cannot be discarded entirely because of its shortcomings. FSO finds potential applications in inter-satellite, orbit to the ground station (GS) and GS to orbit communication [4]. There have been various research and developments carried out by different space agencies [5] , [6], [7]. Near-Earth links have shown the potential to support high data rates greater than 1 Gb/s for the space-to-ground link, and 5.6 Gb/s for space-to-space and ground-to-space links [8]. Moreover, different techniques like aperture averaging [9] and use of HAPS as a relay for a single link FSO system for SATCOM are proposed in various works [10], [11], [12] to overcome some of the limitations of FSO link.

The FSO and RF link is not affected by the atmospheric and weather condition the same way. Studies [13] have shown that the RF link has more susceptibility towards heavy rain and oxygen absorption as compared to the FSO link, and has little or no effect from the fog. While in the case of the FSO link, fog is seen to be the main degrading factor [3]. However, rain does not affect the reliability of the FSO link significantly [3]. Moreover, this complimentary behaviour of FSO and RF links has led to the development and analysis of effective switching schemes for the hybrid FSO/RF systems. These systems exploit the high data transfer rate of FSO link but still are reliable enough for long-distance communication which can cater to the needs of different communication environments such as SATCOM and terrestrial communication.

One approach is to switch between the RF and FSO link to use their complementary natures. However this approach requires constant hardware switching [14], [15]. Another approach is to continuously send data over both the links and use combining techniques at the receiver [13]. But in this method, we are not using the FSO link at its highest data carrying capability because of simultaneous transmission of data over the RF link which operates at a lower data rate. And due to simultaneous transmission, the power is wasted over RF link even if the FSO link provides a good communication link. Adaptive combining based switching (ACBS) [16] provides better utilisation of FSO link. In ACBS FSO link is used as a primary link over which the data is transmitted continuously, while RF is used only as a backup link and MRC combining is used at the receiver when RF link is active.

The RF link for a SATCOM communication is believed to have a direct line of sight component or a strong path due to the presence of fewer scattering elements as compared to the terrestrial communication, where the presence of multiple scattering components, like buildings in an urban setup, are high. Ricean fading, which is having non-zero mean, models this characteristic of SATCOM RF link. While in the case of the FSO channel, the atmospheric turbulence caused by solar heating and wind leads to variations in the refractive index of the air along the transmission path. This causes random fluctuations in both the amplitude and phase of the received signal. This results in considerable degradation of the system performance. The stochastic model used to model the atmospheric turbulence-induced fading is the Gamma-Gamma distribution. The model can also incorporate the beam wander induced pointing errors for the uplink scenario, which can be ignored in discussions of the downlink communication [17].

1.1 Motivations

The motivations behind the proposed work are as follows:

- In prior works performance analysis of only single link FSO systems has been carried out for satellite communication (SATCOM) [10].
- In [16], the adaptive-combining based switching scheme is analysed extensively for the single-hop scenario of terrestrial communication. Moreover, the closed-form expressions are derived only for the outage and not for the average symbol error rate (SER).
- There is a need to derive asymptotic expression of the system performance parameters for better computational analysis of diversity order of the system.
- The performance of hybrid FSO/RF based SATCOM for up-link and down-link scenarios has not been investigated in the literature to the best of our knowledge.

1.2 Contributions

The major contribution of our work are as follows:

- The application of ACBS hybrid FSO/RF system is extended to single-hop up-link, i.e. ground station (GS) to low earth orbit (LEO), and down-link (LEO-GS) SATCOM scenario.

- Apart from application in single-hop SATCOM, the analysis has also been extended to a dual-hop scenario where HAPS is used as a relay between the GS and LEO link, i.e. GS-HAPS-LEO and LEO-GS-HAPS.

- The closed-form expressions of the system performance parameters for the single-hop (SH) and dual-hop (DH) hybrid FSO/RF system are derived considering both up-link and down-link SATCOM scenarios and are validated using the Monte-Carlo simulation results.

- Further, asymptotic expressions of the outage and average SER are derived for both the SH and DH hop SATCOM scenario.

Chapter 2

Single hop hybrid FSO/RF system

2.1 System model

In this system, we assume slow and flat fading, where the channel gain remains constant for at least one transmitted symbol period and affects all frequencies and the transmitter has perfect channel state information (CSI).

The received signal by the RF and the FSO systems are given by

$$y_{RF}[k] = h[k]x[k] + n_1[k] \tag{2.1}$$

$$y_{FSO}[k] = I[k]x[k] + n_2[k] \tag{2.2}$$

Where y[k] is the received symbol, x[k] is the transmitted signal, h[k] and I[k] are the channel gain of the RF and FSO systems respectively, and $n_1[k]$ and $n_2[k]$ are the additive white Gaussian noise (AWGN) of the RF and FSO links.

In the adaptive combining based switching ACBS hybrid FSO/RF system, the symbol is transmitted over the single FSO link when the instantaneous signal to noise ratio (SNR) of the FSO system (γ_{FSO}) is above the pre-determined switching threshold (γ_T). And when $\gamma_{FSO} \leq \gamma_T$, the symbol is transmitted over both the FSO and RF links and maximum ratio combining (MRC) is used at the receiver. The combining rule at the receiver is given by

$$y_{mrc} = \frac{\sqrt{\gamma_{RF}}}{\sigma_{n_1}} y_{RF} + \frac{\sqrt{\gamma_{FSO}}}{\sigma_{n_2}} y_{FSO} \tag{2.3}$$

where γ_{RF} is the instantaneous of RF link, σ_{n_2} and σ_{n_2} are the variances of the AWGN of the RF and FSO links. So, based on the definition of ACBS hybrid system, the instantaneous SNR of the system is defined as

$$\gamma_c = \begin{cases} \gamma_{FSO} + \gamma_{RF}, & \gamma_{FSO} < \gamma_T. \\ \gamma_{FSO}, & \gamma_{FSO} \geq \gamma_T. \end{cases} \tag{2.4}$$

To model the instantaneous SNR of the ACBS hybrid system for the analysis of system performance parameters, first, we need to derive the expression of PDF and CDF of instantaneous SNR of the RF and FSO links, which are given in the next section.

2.2 Channel model

2.2.1 RF channel modelling

In SATCOM the due to the presence of a strong line of sight (LOS) component and weak scattered components between the transmitter and receiver as in SATCOM the RF signal has to go through very minimum scattering and reflection from the environment due to which we model the norm of small scale fading channel coefficient ($|h|$) of the RF channel using Ricean distribution [18, Eq. (2.16)]. Ricean distribution has non-zero mean representing the presence of strong LOS component. The relation between γ_{RF} and $|h|$ is given by

$$\gamma_{RF} = \bar{\gamma}_{RF}|h_{RF}|^2, \tag{2.5}$$

where $\bar{\gamma}_{RF}$ is the average SNR of the RF link.

Now using Maclaurin series expansion of Bessel function of the first kind [table of integral] and power transformation of random variables we get the pdf of the instantaneous SNR of the RF link as

$$f_{\gamma_{RF}}(x) = Fe^{-K}\sum_{n=0}^{\infty}\frac{(-F)^n}{n!}\sum_{i=0}^{\infty}\frac{(KF)^i}{(i!)^2}x^{n+i}, \tag{2.6}$$

where K is the Ricean factor and $F = \frac{K+1}{\bar{\gamma}_{RF}}$.

The corresponding CDF of (2.6) is given by

$$F_{\gamma_{\mathrm{RF}}}(x) = Fe^{-K}\sum_{n=0}^{\infty}\frac{(-F)^n}{n!}\sum_{i=0}^{\infty}\frac{(KF)^i}{(i!)^2}\frac{x^{n+i+1}}{n+i+1}, \tag{2.7}$$

2.2.2 FSO channel modeling

The relation between the instantaneous SNR of the FSO system and received optical irradiance or the normalised fading gain of the FSO system (I) is given by

$$\gamma_{FSO} = \bar{\gamma}_{FSO}|I|^2, \tag{2.8}$$

where $\bar{\gamma}_{FSO}$ is the average SNR of the FSO link.

The received optical irradience of the FSO system is modelled using Gamma-Gamma distribution which account for moderate and strong atmospheric turbulence [3]. Now using [19] to represent the Bessel's function in Meijer-G form and using power transformation of random variables we get the PDF of γ_{FSO} as

$$f_{\gamma_{\text{FSO}}}(x) = \frac{x^{-1}}{2\Gamma(\alpha)\Gamma(\beta)} G_{0,2}^{2,0}\left(Dx^{\frac{1}{2}} \mid \begin{matrix} - \\ \alpha, \beta \end{matrix} \right), \tag{2.9}$$

where α and β are the small scale and large scale scattering parameters and $D = \alpha\beta(\bar{\gamma}_{FSO})^{-1/2}$. Refer to [20] for the calculation of α and β in uplink scenario and to [10] for downlink scenario.

The CDF of the (2.9) can be obtained as

$$F_{\gamma_{FSO}}(x) = \frac{2^{\alpha+\beta-2}}{\pi\Gamma(\alpha)\Gamma(\beta)} G_{1,5}^{4,1}\left(\frac{D^2 x}{16} \mid \begin{matrix} 1 \\ b_1, b_2, b_3, b_4, b_5 \end{matrix} \right) \tag{2.10}$$

where $b_1 = \frac{\alpha}{2}, b_2 = \frac{\alpha+1}{2}, b_3 = \frac{\beta}{2}, b_4 = \frac{\beta+1}{2}$ & $b_5 = 0$.

2.3 Performance analysis

In this section, the outage and average symbol error rate (SER) for single-hop (DH) ACBS hybrid FSO/RF system are analysed for an uplink scenario. The closed-form expression will remain the same for both uplink and downlink scenarios. The difference will come only in the α and β. So, this analysis can be extended for downlink by using α and β of the downlink scenario.

2.3.1 Outage analysis

The system is said to be in outage when γ_c falls below a predefined outage threshold SNR (γ_{out}). When the system is in outage, it is not able to support the target bit-error-rate (BER). For outage analysis, we need the CDF of γ_c, and by simply evaluating the CDF of γ_c at γ_{out} we can get the outage probability. Now according to the definition of the ACBS hybrid FSO/RF system the CDF of γ_c can be written as

$$F_{\gamma_c}(x) = Pr[\gamma_{\text{FSO}} \geq \gamma_{\text{T}}, \gamma_{\text{FSO}} < x] + Pr[\gamma_{\text{FSO}} < \gamma_{\text{T}}, \gamma_{\text{FSO}} + \gamma_{\text{RF}} < x] \tag{2.11}$$

Expanding (2.11) we get

$$F_{\gamma_c}(x) = \begin{cases} F_1(x), & x \leq \gamma_{\text{T}}. \\ F_2(x) - F_{\gamma_{\text{FSO}}}(\gamma_T) + F_{\gamma_{\text{FSO}}}(x), & x > \gamma_{\text{T}}. \end{cases} \tag{2.12}$$

where

$$F_1(x) = \int_0^x f_{\gamma_{FSO}+\gamma_{RF}}(t)dt \tag{2.13}$$

and

$$F_2(x) = \int_0^{\gamma_T} f_{\gamma_{FSO}}(t) F_{\gamma_{RF}}(x-t)dt \tag{2.14}$$

$f_{\gamma_{FSO}+\gamma_{RF}}$ can be calculated using the fact that the FSO and RF links are statistically independent of each other. Which gives us

$$f_{\gamma_{FSO}+\gamma_{RF}}(x) = \int_0^x f_{\gamma_{FSO}}(t) f_{\gamma_{RF}}(x-t)dt \tag{2.15}$$

On substituting (2.6) and (2.9) in (2.15) and using [21, Eq. (07.34.21.0084.01)] we get

$$f_{\gamma_{FSO}+\gamma_{RF}}(x) = \frac{2^{\alpha+\beta-2}Fe^{-K}}{\pi\Gamma(\alpha)\Gamma(\beta)} \sum_{n=0}^{\infty} \frac{(-Fx)^n}{n!} \sum_{i=0}^{\infty} \frac{(KFx)^i}{(i!)^2} \Gamma(n+i+1) \times G_{1,5}^{4,1}\left(\frac{D^2x}{16} \middle| \begin{matrix} 1 \\ \mathscr{B}_6 \end{matrix} \right), \tag{2.16}$$

where $\mathscr{B}_6 = [\mathscr{B}_{6,1}, \mathscr{B}_{6,2}, \mathscr{B}_{6,3}, \mathscr{B}_{6,4}, \mathscr{B}_{6,5}] = [\frac{\alpha}{2}, \frac{\alpha+1}{2}, \frac{\beta}{2}, \frac{\beta+1}{2}, -n-i]$.

By substituting (2.16) in (2.13) and using [21, Eq. (07.34.21.0084.01)] we get

$$F_1(x) = \frac{2^{\alpha+\beta-2}Fxe^{-K}}{\pi\Gamma(\alpha)\Gamma(\beta)} \sum_{n=0}^{\infty} \frac{(-Fx)^n}{n!} \sum_{i=0}^{\infty} \frac{(KFx)^i}{(i!)^2} \Gamma(n+i+1) \times G_{2,6}^{4,2}\left(\frac{D^2x}{16} \middle| \begin{matrix} \mathscr{B}_7 \\ \mathscr{B}_8 \end{matrix} \right), \tag{2.17}$$

where $\mathscr{B}_7 = [\mathscr{B}_{7,1}, \mathscr{B}_{7,2}] = [-n-i, 1]$ and
$\mathscr{B}_8 = [\mathscr{B}_{8,1}, \mathscr{B}_{8,2}, \mathscr{B}_{8,3}, \mathscr{B}_{8,4}, \mathscr{B}_{8,5}, \mathscr{B}_{8,6}] = [\frac{\alpha}{2}, \frac{\alpha+1}{2}, \frac{\beta}{2}, \frac{\beta+1}{2}, -n-i, -n-i-1]$.

Similarly we can calculate $F_2(x)$ by substituting (2.7) and (2.9) in (2.14). After applying binomial expansion and using [21, Eq. (07.34.21.0084.01)] we get

$$F_2(x) = \frac{2^{\alpha+\beta-2}Fxe^{-K}}{\pi\Gamma(\alpha)\Gamma(\beta)} \sum_{n=0}^{\infty} \frac{(-Fx)^n}{n!} \sum_{i=0}^{\infty} \frac{(KFx)^i}{(i!)^2(n+i+1)} \sum_{p=0}^{n+i+1} \binom{n+i+1}{p} \left(\frac{-\gamma_T}{x} \right)^p \times G_{1,5}^{4,1}\left(\frac{D^2\gamma_T}{16} \middle| \begin{matrix} \mathscr{B}_9 \\ \mathscr{B}_{10} \end{matrix} \right), \tag{2.18}$$

where $\mathscr{B}_9 = [\mathscr{B}_{9,1}] = [1-p]$ and $\mathscr{B}_{10} = [\mathscr{B}_{10,1}, \mathscr{B}_{10,2}, \mathscr{B}_{10,3}, \mathscr{B}_{10,4}, \mathscr{B}_{10,5}] = [\frac{\alpha}{2}, \frac{\alpha+1}{2}, \frac{\beta}{2}, \frac{\beta+1}{2}, -p]$. Substituting (2.17), (2.18) and (2.10) in (2.12), we obtain $F_{\gamma_c}(x)$. We can determine P_{AC} using $F_{\gamma_c}(\gamma_{out})$.

2.3.2 Average symbol error rate

The conditional probability of error for an M-arr PSK system is given by

$$P(e|x) = \frac{A}{2} erfc(\sqrt{x}B) \tag{2.19}$$

where $erfc(.)$ is the complimetary error function, x is the instantaneous SNR of the MPSK system, $B = sin(\frac{\pi}{M})$ and

$$A = \begin{cases} 1, & M = 2. \\ 2, & M > 2. \end{cases} \tag{2.20}$$

Maclaurin series of $P(e|x)$

$$P(e|x) = \frac{A}{2}\left[1 - \frac{2}{\sqrt{\pi}} \sum_{p=0}^{\infty} \frac{(-1)^p x^{\frac{(2p+1)}{2}} B^{(2p+1)}}{p!(2p+1)}\right] \tag{2.21}$$

and Meijer-G representations of $P(e|x)$ is

$$P(e|x) = \frac{A}{2\sqrt{\pi}} G_{1,2}^{2,0}\left(\frac{B^2 x}{16} \mid \begin{matrix} 1 \\ 0, \frac{1}{2} \end{matrix}\right) \tag{2.22}$$

The average SER of the ACBS hybrid FSO/RF system can be calculated by averaging the conditional error probability over the PDF of γ_c. So, we need to determine the PDF of γ_c ($f_{\gamma_c}(x)$). $f_{\gamma_c}(x)$ can be obtained by differentiating the CDF of γ_c. On differentiating (2.12) with respect to x we get.

$$f_{\gamma_c}(x) = \begin{cases} f_{\gamma_{FSO}+\gamma_{RF}}(x), & x \leq \gamma_{\mathrm{T}}. \\ G(x) + f_{\gamma_{\mathrm{FSO}}}(x), & x > \gamma_{\mathrm{T}}. \end{cases} \tag{2.23}$$

where

$$G(x) = \int_0^{\gamma_T} f_{\gamma_{FSO}}(t) f_{\gamma_{RF}}(x-t) dt \tag{2.24}$$

On substituting (2.9) and (2.6) in (2.24). Using binomial expansion and [21, Eq. (07.34.21.0084.01)] we get

$$G(x) = \frac{2^{\alpha+\beta-2} F e^{-K}}{\pi\Gamma(\alpha)\Gamma(\beta)} \sum_{n=0}^{\infty} \frac{(-Fx)^n}{n!} \sum_{i=0}^{\infty} \frac{(KFx)^i}{(i!)^2} \sum_{p=0}^{n+i} \binom{n+i}{l} \left(\frac{-\gamma_t}{x}\right)^l G_{1,5}^{4,1}\left(\frac{D^2\gamma_T}{16} \mid \begin{matrix} \mathscr{B}_{11} \\ \mathscr{B}_{12} \end{matrix}\right) \tag{2.25}$$

where $\mathscr{B}_{11} = [\mathscr{B}_{11,1}] = [1-l]$ and $\mathscr{B}_{12} = [\mathscr{B}_{12,1}, \mathscr{B}_{12,2}, \mathscr{B}_{12,3}, \mathscr{B}_{12,4}, \mathscr{B}_{12,5}] = [\frac{\alpha}{2}, \frac{\alpha+1}{2}, \frac{\beta}{2}, \frac{\beta+1}{2}, -l]$

By definition, the average SER of the system can now be calculated as

$$\bar{P_e}^{AC} = \int_0^{\infty} \frac{A}{2} erfc(\sqrt{x}B) f_{\gamma_c}(x) dx \tag{2.26}$$

substituting (2.23) in (2.26) we get

$$\begin{aligned}\bar{P}_e^{AC} &= \underbrace{\int_0^{\gamma_T} P(e|x) f_{\gamma_{FSO}+\gamma_{RF}}(x)dx}_{\mathrm{I_1}} + \underbrace{\int_{\gamma_T}^{\infty} P(e|x)(f_{\gamma_{FSO}}(x)+G(x))dx}_{\mathrm{I_2}} \\ &= I_1 + I_2\end{aligned} \tag{2.27}$$

where

$$I_1 = \int_0^{\gamma_T} erfc(\sqrt{x}B) f_{\gamma_{FSO}+\gamma_{RF}}(x)dx \tag{2.28}$$

on substituting (2.16) and (2.21) in (2.28). And using [21, Eq. (07.34.21.0084.01)] we get

$$\begin{aligned}I_1 = F_1(\gamma_T) - \frac{2^{\alpha+\beta-2} A F \gamma_T^{\frac{3}{2}} e^{-K}}{\pi^{\frac{3}{2}} \Gamma(\alpha)\Gamma(\beta)} \Bigg[\sum_{n=0}^{\infty} \frac{(-F\gamma_T)^n}{n!} \sum_{i=0}^{\infty} \frac{(KF\gamma_T)^i}{(i!)^2} \Gamma(n+i+1) \\ \times \sum_{p=0}^{n+i} \frac{(-\gamma_t) B^{(2l+1)^l}}{l!(2l+1)} G_{2,6}^{4,2}\left(\frac{D^2\gamma_T}{16} \,\middle|\, \begin{matrix} \mathscr{B}_{13} \\ \mathscr{B}_{14} \end{matrix} \right) \Bigg]\end{aligned} \tag{2.29}$$

where $\mathscr{B}_{13} = [\mathscr{B}_{13,1}, \mathscr{B}_{13,2}] = [(\frac{1}{2} - n - i - l), 1]$ and
$\mathscr{B}_{14} = [\mathscr{B}_{14,1}, \mathscr{B}_{14,2}, \mathscr{B}_{14,3}, \mathscr{B}_{14,4}, \mathscr{B}_{14,5}, \mathscr{B}_{14,6}] = [\frac{\alpha}{2}, \frac{\alpha+1}{2}, \frac{\beta}{2}, \frac{\beta+1}{2}, -n-i, -n-i-l-\frac{3}{2}]$.

I_2 can be calculated using

$$I_2 = \int_{\gamma_T}^{\infty} P(e|x) f_{\gamma_{FSO}}(x)dx + \underbrace{\int_{\gamma_T}^{\infty} P(e|x) G(x)dx}_{\mathrm{I_{23}}} \tag{2.30}$$

on directly evaluating (2.30) we get a form which has convergence issues while analysing it using MATLAB. So, we use the property of integral to change the limits of integration in (2.30) as

$$\begin{aligned}I_2 &= \underbrace{\int_0^{\infty} P(e|x) f_{\gamma_{FSO}}(x)dx}_{\mathrm{H}} - \int_0^{\gamma_T} P(e|x) f_{\gamma_{FSO}}(x)dx + I_{23} \\ &= \underbrace{H - \frac{A}{2} F_{\gamma_{FSO}}(\gamma_T)}_{\mathrm{I_{21}}} + \underbrace{\frac{A}{2}\int_0^{\gamma_T} erf(\sqrt{x}B) f_{\gamma_{FSO}}(x)dx}_{\mathrm{I_{22}}} + I_{23}\end{aligned} \tag{2.31}$$

where erf(.), H is the average SER of FSO link. H is given as

$$H = \frac{2^{\alpha+\beta}}{8\pi^{3/2}\Gamma(\alpha)\Gamma(\beta)} G_{2,5}^{4,2}\left(\frac{D^2\gamma_T}{4B} \,\middle|\, \begin{matrix} \mathscr{B}_{15} \\ \mathscr{B}_{16} \end{matrix} \right), \tag{2.32}$$

where $\mathscr{B}_{15} = [1, \frac{1}{2}]$ and $\mathscr{B}_{16} = [\mathscr{B}_{16,1}, \mathscr{B}_{16,2}, \mathscr{B}_{16,3}, \mathscr{B}_{16,4}, \mathscr{B}_{16,5}] = [\frac{\alpha}{2}, \frac{\alpha+1}{2}, \frac{\beta}{2}, \frac{\beta+1}{2}, 0]$

I_{22} is evaluated by using Maclaurin series expansion of the error function and by substituting (2.9) in (2.31) and using [21, Eq. (07.34.21.0084.01)]

$$I_{22} = \frac{2^{\alpha+\beta-1}}{\pi^{3/2}\Gamma(\alpha)\Gamma(\beta)} \sum_{n=0}^{\infty} \frac{(-1)^n (B\sqrt{\gamma_T})^{2n+1}}{n!(2n+1)} G_{1,5}^{4,1}\left(\frac{D^2\gamma_T}{16} \,\middle|\, \begin{matrix} \mathscr{B}_{17} \\ \mathscr{B}_{18} \end{matrix} \right), \tag{2.33}$$

where $\mathscr{B}_{17} = [\frac{1}{2} - n]$ and $\mathscr{B}_{18} = [\mathscr{B}_{18,1}, \mathscr{B}_{18,2}, \mathscr{B}_{18,3}, \mathscr{B}_{18,4}, \mathscr{B}_{18,5}] = [\frac{\alpha}{2}, \frac{\alpha+1}{2}, \frac{\beta}{2}, \frac{\beta+1}{2}, -n - \frac{1}{2}]$

I_{23} is obtained by using (2.22), (2.25) in (2.30), and integrating it using [21, Eq. (07.34.21.0085.01)]

$$I_{23} = \frac{2^{\alpha+\beta-3} F \gamma_T e^{-K}}{\pi^{\frac{3}{2}} \Gamma(\alpha)\Gamma(\beta)} \sum_{n=0}^{\infty} \frac{(-F\gamma_T)^n}{n!} \sum_{i=0}^{\infty} \frac{(KF\gamma_T)^i}{(i!)^2} \sum_{p=0}^{n+i} \binom{n+i}{l} (-1)^l$$
$$G_{1,5}^{4,1}\left(\frac{D^2 \gamma_T}{16} \mid \begin{matrix} \mathscr{B}_{11} \\ \mathscr{B}_{12} \end{matrix} \right) G_{3,0}^{2,3}\left(B^2 \gamma_T \mid \begin{matrix} \mathscr{B}_{19} \\ \mathscr{B}_{20} \end{matrix} \right) \tag{2.34}$$

where$\mathscr{B}_{19}$ = $[\mathscr{B}_{19,1}, \mathscr{B}_{19,2}, \mathscr{B}_{19,3}]$ =$[l-n-i-1, 0, \frac{1}{2}]$ and $\mathscr{B}_{20}$ = $[\mathscr{B}_{20,1}, \mathscr{B}_{20,2}]$ = $[1, l-n-i]$

On substituting (2.10), (2.32), (2.33) and (2.34) in (2.31) we get I_2 and on substituting the value of I_2 and (2.28) in (2.27) we can get the average SER of the single hop system.

Chapter 3

Dual-hop hybrid FSO/RF system

Chapter 1 discussed the system model, outage and average SER analysis of single-hop ACBS hybrid FSO/RF system. In this chapter, we will discuss the system model for dual-hop (DH) ACBS hybrid FSO/RF system and performance analysis of ACBS hybrid FSO/RF system.

3.1 System model

In the dual-hop scenario, we add a relay between the ground station and the low earth orbit (LEO) satellite. We use HAPS stationed at the height of around 21 Km as the relay. Addition of relay breaks the link in two parts — first, the GS-HAPS link and second, the HAPS-LEO link. The relay uses a decode and forward protocol. For the case of transmission between GS and HAPS, the FSO beam is highly susceptible to the atmospheric turbulence, and this makes it necessary to back the FSO link by a reliable RF link and use the ACBS scheme. While the HAPS-LEO link is connected using only a single link FSO system as FSO beam has to go through minimal turbulence in this part of communication. Using the expressions of outage and average SER of ACBS hybrid FSO/RF system derived in the previous chapter, we can obtain the outage and average SER expressions for dual-hop ACBS hybrid FSO RF system.

3.2 Performance analysis

In this section, the outage and average symbol error rate (SER) for single-hop (DH) ACBS hybrid FSO/RF system are analysed for an uplink scenario. The closed-form expression will remain the same for both uplink and downlink scenarios. The difference will come only in the α and β. So, this analysis can be extended for downlink by using α and β of the downlink scenario. Let, the α_1 and β_1 be the small scale and large scale parameters for GS-HAPS, and α_2 and β_2 for the HAPS-LEO link.

Using the expressions of outage and average SER of ACBS hybrid FSO/RF system derived in the previous chapter, we can obtain the outage and average SER expressions for dual-hop ACBS hybrid FSO RF system.

3.2.1 Outage probability

The dual-hop hybrid FSO/RF system will be in outage if either of the systems used in GS-HAPS link or the HAPS-LEO link is in outage. In other words, the system will not be in outage if both the systems are not in outage. Moreover, this can be evaluated using the fact that the ACBS hybrid FSO/RF system and the single link FSO system are statistically independent of each other. So, the probability that the system is not in outage can be written as

$$Z = (1 - P_{AC})(1 - P_{FSO}) \tag{3.1}$$

where P_{AC} is the outage probability of the ACBS hybrid FSO/RF system and P_{FSO} is the outage probability of the FSO system. P_{FSO} can be derived by substituting the γ_{out}, for the single link FSO system used for GS/HAPS link, in (2.10). The probability of outage of the DH system will be

$$P_{DH} = 1 - Z \tag{3.2}$$

substituting (3.1) in (3.2) we get

$$\begin{aligned} P_{DH} &= 1 - (1 - P_{AC})(1 - P_{FSO}) \\ &= P_{AC} + P_{FSO} - P_{AC} \times P_{FSO} \\ &\approx P_{AC} + P_{FSO} \end{aligned} \tag{3.3}$$

here the negative term can be ignored as its value is very less as compared to the sum of the other two terms. On substituting the value of P_{AC} and P_{FSO} in (3.3), we get the outage probability of the DH ACBS hybrid FSO/RF system.

3.2.2 Average symbol error rate

Average SER of the DH ACBS hybrid FSO/RF system ca be derived in a similar way as the outage probability. We have to consider one system at a time and use the conditional probability of error. So, the signal received at the destination, i.e. LEO satellite for up-link and GS for down-link, will be in error if one of the links, i.e. GS-HAPS or HAPS-LEO is erroneous while the other is not. So, Average SER is

$$\begin{aligned} \bar{P}_e^{DH} &= (1 - H)\bar{P}_e^{AC} + H(1 - \bar{P}_e^{AC}) \\ &= \bar{P}_e^{AC} + H - 2\bar{P}_e^{AC} H \end{aligned} \tag{3.4}$$

where $\bar{P}_e^{AC}$ is the probability of error of the ACBS hybrid FSO/RF system discussed in section (2.3.2) and H is the average bit error rate of the FSO system (2.32). Unlike outage here we cannot ignore the negative term.

Chapter 4

Asymptotic analysis

The asymptotic analysis is carried out to get the diversity order of the system. At higher values of SNR, the asymptotic expression is equal to the closed-form expression. This property is used to get the slope of the closed-form expressions at higher values of the SNR. At higher values of SNR the closed-form expressions of the performance parameters can be expressed in the form $(G_c SNR)^{-G_d}$ where G_d and G_c are the diversity gain and coding gain of the system. We assume $\bar{\gamma}_{FSO}$ tends to infinity to derive the asymptotic expressions.

As $\bar{\gamma}_{FSO} \implies \infty$, $D \implies 0$, using the expansion to Meijer-G funtion for input argument tending to zero [21, Eq. (07.34.06.0040.01)], we get the asymptotic expressions of the system performance parameters.

4.1 Outage probability

4.1.1 Single-hop

As $\bar{\gamma}_{FSO} \implies \infty$, $P_{AC} \implies P_{AC}^{asy}$. For $\gamma_{out} \leq \gamma_T$ it is given by

$$P_{AC}^{asy} = \frac{2^{\alpha+\beta-2} F \gamma_{out} e^{-K}}{\pi\Gamma(\alpha)\Gamma(\beta)} \sum_{n=0}^{\infty} \frac{(-F\gamma_{out})^n}{n!} \sum_{i=0}^{\infty} \frac{(KF\gamma_{out})^i}{(i!)^2} \Gamma(n+i+1)\mathscr{C}_1, \tag{4.1}$$

where

$$\mathscr{C}_1 = \sum_{k=1}^{4} \frac{\prod_{\substack{j=1\\j\neq k}}^{4} \Gamma(\mathscr{B}_{8,j} - \mathscr{B}_{8,k}) \prod_{j=1}^{2} \Gamma(1 - \mathscr{B}_{7,j} + \mathscr{B}_{8,k})}{\prod_{j=5}^{6} \Gamma(1 - \mathscr{B}_{8,j} + \mathscr{B}_{8,k})} \times \left(\frac{D^2 \gamma_{out}}{16}\right)^{\mathscr{B}_{8,k}}$$

and for $\gamma_{out} > \gamma_T$,

$$P_{AC}^{asy} = \frac{2^{\alpha+\beta-2}}{\pi\Gamma(\alpha)\Gamma(\beta)} \Bigg[\mathscr{C}_2 - \mathscr{C}_3 + \Bigg\{F\gamma_{out} e^{-K} \sum_{n=0}^{\infty} \frac{(-F\gamma_{out})^n}{n!} \sum_{i=0}^{\infty} \frac{(KF\gamma_{out})^i}{(i!)^2 (n+i+1)} \times \sum_{p=0}^{n+i+1} \binom{n+i+1}{p} \left(\frac{-\gamma_T}{\gamma_{out}}\right)^p \mathscr{C}_4 \Bigg\}\Bigg], \tag{4.2}$$

where

$$\mathscr{C}_2 = \sum_{k=1}^{4} \frac{\prod_{\substack{j=1\\ j\neq k}}^{4} \Gamma(b_j - b_k)}{b_k} \left(\frac{D^2 \gamma_{out}}{16}\right)^{b_k}, \tag{4.3}$$

$$\mathscr{C}_3 = \sum_{k=1}^{4} \frac{\prod_{\substack{j=1\\ j\neq k}}^{4} \Gamma(b_j - b_k)}{b_k} \left(\frac{D^2 \gamma_{T}}{16}\right)^{b_k} \tag{4.4}$$

and

$$\mathscr{C}_4 = \sum_{k=1}^{4} \frac{\prod_{\substack{j=1\\ j\neq k}}^{4} \Gamma(\mathscr{B}_{10,j} - \mathscr{B}_{10,k})}{p + \mathscr{B}_{10,k}} \left(\frac{D^2 \gamma_{T}}{16}\right)^{\mathscr{B}_{10,k}} \tag{4.5}$$

4.1.2 Dual-hop

As $\bar{\gamma}_{FSO} \implies \infty$, $P_{DH} \implies P_{DH}^{asy}$. For $\gamma_{out} \leq \gamma_T$ is given by

$$\begin{aligned} P_{DH}^{asy} &= P_{AC}^{asy} + P_{FSO}^{asy} \\ &= \frac{2^{\alpha_2+\beta_2-2}}{\pi\Gamma(\alpha_2)\Gamma(\beta_2)}\mathscr{C}_5 + \frac{2^{\alpha_1+\beta_1-2} F\gamma_{out} e^{-K}}{\pi\Gamma(\alpha_1)\Gamma(\beta_1)} [\sum_{n=0}^{\infty} \frac{(-F\gamma_{out})^n}{n!} \sum_{i=0}^{\infty} \frac{(KF\gamma_{out})^i}{(i!)^2} \Gamma(n+i+1)\mathscr{C}_6, \end{aligned} \tag{4.6}$$

$$\mathscr{C}_5 = \sum_{k=1}^{4} \frac{\prod_{\substack{j=1\\ j\neq k}}^{4} \Gamma(b_j - b_k)}{b_k} \left(\frac{D^2 \gamma_{out}}{16}\right)^{b_k}, \tag{4.7}$$

$$\mathscr{C}_6 = \sum_{k=1}^{4} \frac{\prod_{\substack{j=1\\ j\neq k}}^{4} \Gamma(\mathscr{B}_{8,j} - \mathscr{B}_{8,k}) \prod_{j=1}^{2} \Gamma(1 - \mathscr{B}_{7,j} + \mathscr{B}_{8,k})}{\prod_{j=5}^{6} \Gamma(1 - \mathscr{B}_{8,j} + \mathscr{B}_{8,k})} \times \left(\frac{D^2 \gamma_{out}}{16}\right)^{\mathscr{B}_{8,k}}$$

as α_2 and β_2 are of the order of 10^4 the first term i.e. the term involving $\mathscr{C}_5$ is ignored. So P_{DH}^{asy} is approximately equal to

$$P_{DH}^{asy} = \frac{2^{\alpha_1+\beta_1-2} F\gamma_{out} e^{-K}}{\pi\Gamma(\alpha_1)\Gamma(\beta_1)} \sum_{n=0}^{\infty} \frac{(-F\gamma_{out})^n}{n!} \sum_{i=0}^{\infty} \frac{(KF\gamma_{out})^i}{(i!)^2} \Gamma(n+i+1)\mathscr{C}_6, \tag{4.8}$$

For $\gamma_{out} > \gamma_T$,

$$\begin{aligned} P_{AC}^{asy} = \frac{2^{\alpha_2+\beta_2-2}}{\pi\Gamma(\alpha_2)\Gamma(\beta_2)}\mathscr{C}_7 + \frac{2^{\alpha_1+\beta_1-2}}{\pi\Gamma(\alpha_1)\Gamma(\beta_1)} \Bigg[\mathscr{C}_8 - \mathscr{C}_9 + \Bigg\{ F\gamma_{out} e^{-K} \sum_{n=0}^{\infty} \frac{(-F\gamma_{out})^n}{n!} \sum_{i=0}^{\infty} \frac{(KF\gamma_{out})^i}{(i!)^2 (n+i+1)} \\ \times \sum_{p=0}^{n+i+1} \binom{n+i+1}{p} \left(\frac{-\gamma_T}{\gamma_{out}}\right)^p \mathscr{C}_{10} \Bigg\}\Bigg], \end{aligned} \tag{4.9}$$

where

$$\mathscr{C}_7 = \sum_{k=1}^{4} \frac{\prod_{\substack{j=1\\ j\neq k}}^{4} \Gamma(b_j - b_k)}{b_k} \left(\frac{D^2 \gamma_{out}}{16}\right)^{b_k}, \tag{4.10}$$

$$\mathscr{C}_8 = \sum_{k=1}^{4} \frac{\prod_{\substack{j=1\\ j\neq k}}^{4} \Gamma(b_j - b_k)}{b_k} \left(\frac{D^2 \gamma_{out}}{16}\right)^{b_k}, \tag{4.11}$$

,

$$\mathscr{C}_9 = \sum_{k=1}^{4} \frac{\prod_{\substack{j=1\\ j\neq k}}^{4} \Gamma(b_j - b_k)}{b_k} \left(\frac{D^2 \gamma_T}{16}\right)^{b_k} \tag{4.12}$$

and

$$\mathscr{C}_{10} = \sum_{k=1}^{4} \frac{\prod_{\substack{j=1\\ j\neq k}}^{4} \Gamma(\mathscr{B}_{10,j} - \mathscr{B}_{10,k})}{p + \mathscr{B}_{10,k}} \left(\frac{D^2 \gamma_T}{16}\right)^{\mathscr{B}_{10,k}} \tag{4.13}$$

Similarly, the term involving $\mathscr{C}_7$ as α_2 and β_2 are of the order of 10^4.

$$P_{AC}^{asy} = \frac{2^{\alpha_1+\beta_1-2}}{\pi\Gamma(\alpha_1)\Gamma(\beta_1)} \Bigg[\mathscr{C}_8 - \mathscr{C}_9 + \Bigg\{ F\gamma_{out} e^{-K} \sum_{n=0}^{\infty} \frac{(-F\gamma_{out})^n}{n!} \sum_{i=0}^{\infty} \frac{(KF\gamma_{out})^i}{(i!)^2(n+i+1)} \times \sum_{p=0}^{n+i+1} \binom{n+i+1}{p} \left(\frac{-\gamma_T}{\gamma_{out}}\right)^p \mathscr{C}_{10} \Bigg\}\Bigg], \tag{4.14}$$

4.2 Average SER

Similar to the outage asymptotic expression in this section, we derive the asymptotic expression of the average SER using the fact that $\bar{\gamma}_{FSO} \implies \infty$, $D \implies 0$. Using [21, Eq. (07.34.06.0040.01)] to replace the Meijer-G with the series, we can derive the asymptotic expression of the average SER

4.2.1 Single-hop

As $\bar{\gamma}_{FSO} \implies \infty$, $\bar{P}_e^{AC} \implies \bar{P}_e^{ACasy}$, $I_1 \implies I_1^{asy}$, $I_2 \implies I_2^{asy}$, $F_1(\gamma_T) \implies F_1^{asy}(\gamma_T)$, $H \implies H^{asy}$, $F_{\gamma_{FSO}}(\gamma_T) \implies F_{\gamma_{FSO}}^{asy}(\gamma_T)$, $I_{22} \implies I_{22}^{asy}$, $I_{23} \implies I_{23}^{asy}$. So from equation (2.27) we get

$$\bar{P}_e^{ACasy} = I_1^{asy} + I_2^{asy} \tag{4.15}$$

From (2.28), (2.17) and [21, Eq. (07.34.06.0040.01)] we get the asymptotic expression of I_1 as

$$I_1^{asy} = F_1^{asy}(\gamma_T) - \frac{2^{\alpha+\beta-2} A F \gamma_T^{\frac{3}{2}} e^{-K}}{\pi^{\frac{3}{2}}\Gamma(\alpha)\Gamma(\beta)} \Bigg[\sum_{n=0}^{\infty} \frac{(-F\gamma_T)^n}{n!} \sum_{i=0}^{\infty} \frac{(KF\gamma_T)^i}{(i!)^2} \Gamma(n+i+1) \times \sum_{p=0}^{n+i} \frac{(-\gamma_t) B^{(2l+1)^l}}{l!(2l+1)} \times \mathscr{C}_{11}\Bigg] \tag{4.16}$$

where

$$\mathscr{C}_{11} = \sum_{k=1}^{4} \frac{\prod_{\substack{j=1\\ j\neq k}}^{4} \Gamma(\mathscr{B}_{14,j} - \mathscr{B}_{14,k}) \prod_{j=1}^{2} \Gamma(1 - \mathscr{B}_{13,j} + \mathscr{B}_{14,k})}{\prod_{j=5}^{6} \Gamma(1 - \mathscr{B}_{14,j} + \mathscr{B}_{14,k})} \times \left(\frac{D^2 \gamma_T}{16}\right)^{\mathscr{B}_{14,k}}$$

and

$$F_1^{asy}(\gamma_T) = \frac{2^{\alpha+\beta-2} F x e^{-K}}{\pi\Gamma(\alpha)\Gamma(\beta)} \sum_{n=0}^{\infty} \frac{(-Fx)^n}{n!} \sum_{i=0}^{\infty} \frac{(KFx)^i}{(i!)^2} \Gamma(n+i+1) \times \mathscr{C}_{12} \tag{4.17}$$

where

$$\mathscr{C}_{12} = \sum_{k=1}^{4} \frac{\prod_{\substack{j=1 \\ j\neq k}}^{4} \Gamma(\mathscr{B}_{8,j} - \mathscr{B}_{8,k}) \prod_{j=1}^{2} \Gamma(1 - \mathscr{B}_{7,j} + \mathscr{B}_{8,k})}{\prod_{j=5}^{6} \Gamma(1 - \mathscr{B}_{8,j} + \mathscr{B}_{8,k})} \times \left(\frac{D^2\gamma_T}{16}\right)^{\mathscr{B}_{8,k}} \tag{4.18}$$

On substituting (2.10), (2.32) in (2.31) we get

$$I_2 = H^{asy} - \frac{A}{2} F^{asy}_{\gamma_{FSO}(\gamma_T)} + I_{22}^{asy} + I_{23}^{asy} \tag{4.19}$$

using (2.32), (2.10),(2.33),(2.34) and [21, Eq. (07.34.06.0040.01)]

$$H = \frac{2^{\alpha+\beta}}{8\pi^{3/2}\Gamma(\alpha)\Gamma(\beta)} \times \mathscr{C}_{13}, \tag{4.20}$$

$$F_{\gamma_{FSO}}(x) = \frac{2^{\alpha+\beta-2}}{\pi\Gamma(\alpha)\Gamma(\beta)} \times \mathscr{C}_{14} \tag{4.21}$$

$$I_{22} = \frac{2^{\alpha+\beta-1}}{\pi^{3/2}\Gamma(\alpha)\Gamma(\beta)} \sum_{n=0}^{\infty} \frac{(-1)^n (B\sqrt{\gamma_T})^{2n+1}}{n!(2n+1)} \times \mathscr{C}_{15}, \tag{4.22}$$

$$I_{23} = \frac{2^{\alpha+\beta-3} F\gamma_T e^{-K}}{\pi^{\frac{3}{2}}\Gamma(\alpha)\Gamma(\beta)} \sum_{n=0}^{\infty} \frac{(-F\gamma_T)^n}{n!} \sum_{i=0}^{\infty} \frac{(KF\gamma_T)^i}{(i!)^2} \sum_{p=0}^{n+i} \binom{n+i}{l} (-1)^l \tag{4.23}$$

$$G_{3,0}^{2,3}\left(B^2\gamma_T \,\middle|\, \begin{matrix} \mathscr{B}_{19} \\ \mathscr{B}_{20} \end{matrix}\right) \times \mathscr{C}_{16}$$

where

$$\mathscr{C}_{13} = \sum_{k=1}^{4} \frac{\prod_{\substack{j=1 \\ j\neq k}}^{4} \Gamma(\mathscr{B}_{16,j} - \mathscr{B}_{16,k}) \prod_{j=1}^{2} \Gamma(1 - \mathscr{B}_{15,j} + \mathscr{B}_{16,k})}{\Gamma(1 + \mathscr{B}_{16,k})} \times \left(\frac{D^2\gamma_T}{16}\right)^{\mathscr{B}_{16,k}} \tag{4.24}$$

$$\mathscr{C}_{14} = \sum_{k=1}^{4} \frac{\prod_{\substack{j=1 \\ j\neq k}}^{4} \Gamma(b_j - b_k)}{b_k} \left(\frac{D^2\gamma_T}{16}\right)^{b_k} \tag{4.25}$$

$$\mathscr{C}_{15} = \sum_{k=1}^{4} \frac{\prod_{\substack{j=1 \\ j\neq k}}^{4} \Gamma(\mathscr{B}_{18,j} - \mathscr{B}_{18,k}) \Gamma(1 - \mathscr{B}_{17} + \mathscr{B}_{18,k})}{\Gamma(1 - \mathscr{B}_{18,5} + \mathscr{B}_{18,k})} \times \left(\frac{D^2\gamma_T}{16}\right)^{\mathscr{B}_{18,k}} \tag{4.26}$$

$$\mathscr{C}_{16} = \sum_{k=1}^{4} \frac{\prod_{\substack{j=1 \\ j\neq k}}^{4} \Gamma(\mathscr{B}_{12,j} - \mathscr{B}_{12,k}) \Gamma(1 - \mathscr{B}_{11} + \mathscr{B}_{12,k})}{\Gamma(1 - \mathscr{B}_{12,5} + \mathscr{B}_{12,k})} \times \left(\frac{D^2\gamma_T}{16}\right)^{\mathscr{B}_{12,k}} \tag{4.27}$$

4.2.2 Dual-hop

In the case of the dual-hoop scenario, as discussed earlier, the small scale and large scale parameters are of the order 10^4 for the HAPS-LEO link, and this makes the asymptotic expression of average SER for the single link FSO system between HAPS-LEO negligible as compared to the average SER of ACBS system. So, the asymptotic expression of the average SER for dual-hop scenario becomes equal to the single-hop case. The only difference that comes is the small scale and large scale parameters. Here, α and β correspond to GS-HAPS link, which will have larger magnitude compared to single-hop scenario. Hence, improvement in performance will be obtained for dual-hop scenario with decrease in atmospheric turbulence.

4.3 Conclusion

The expressions derived in sections (4.1) and (4.2) give us an insight into a diversity order of the outage and average SER expressions of the single-hop and dual-hop systems. From sections (4.1) and (4.2) we can see that the asymptotic expressions are of the form $\sum(G_d SNR)^{G_c}$, where the dominant values of G_c are $\left\{\frac{\alpha}{2}, \frac{\alpha+}{2}, \frac{\beta}{2}, \frac{\beta+1}{2}\right\}$ for both the outage and average SER cases as can be seen from the expressions of $\mathscr{C}_1$ to $\mathscr{C}_{16}$.

Chapter 5

Numerical results and discussions

In this chapter, we will analyse the closed-form expressions derived in the earlier chapters. The system parameters used for the analysis are listed in the table (5.1). Unless otherwise stated, the system parameters will be the same as listed in (5.1). The summation limits n, and i are set to be 20 and 20 for analytical analysis. Further increment in the values of n and i does not affect the fifth decimal figure of the outage and average SER.

Table 5.1: Simulation parameters

Outage analysis	
Parameter	**Value**
Ricean factor (K)	1
Switching Threshold (γ_T)	8 dB
Outage Threshold (γ_{out})	3 dB
Lower Earth Orbit Height (H)	620 km
HAPS height (H_{HAPS})	25 km
Average RF SNR ($\bar{\gamma}_{RF}$)	15 dB
Wind Speed (w)	21 m/sec
Zenith Angle (ϕ_{zenith})	80$^{\text{o}}$

Average SER analysis	
Parameter	**Value**
Ricean factor (K)	1
Switching Threshold (γ_T)	5 dB
Outage Threshold (γ_{out})	3 dB
Lower Earth Orbit Height (H)	620 km
HAPS height (H_{HAPS})	25 km
Average RF SNR ($\bar{\gamma}_{RF}$)	27 dB
Wind Speed (w)	21 m/sec
Zenith Angle (ϕ_{zenith})	80$^{\text{o}}$

5.1 System performance analysis

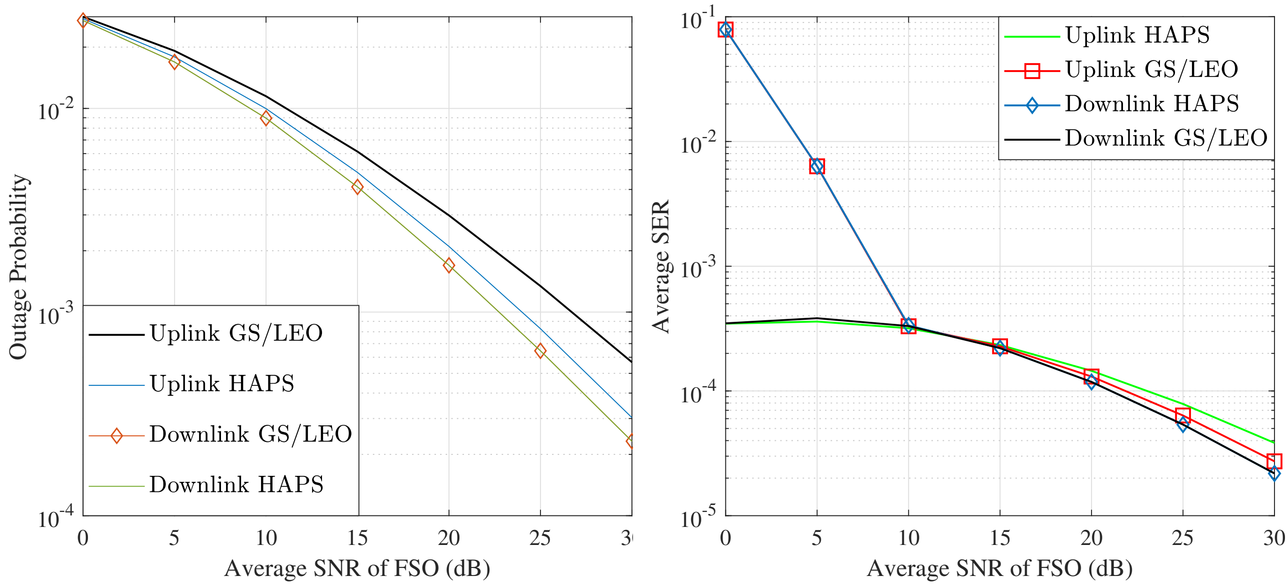

(a) Outage

(b) Average SER

Figure 5.1: System performance parameters vs $\bar{\gamma}_{FSO}$ for up-link and down-link

Here we can see the plots of outage and average SER for up-link and down-link scenario with respect to average SNR of FSO link. From the graph, we can observe that there is a diversity gain in case of the up-link scenarios for the single-hop (GS/LEO) and the dual-hop (HAPS) systems while there is no improvement in the system performance of the dual-hop as compared to the single-hop for the downlink scenario.

In the case of downlink scenario, the data first travels through a low attenuation region. During which it goes through less attenuation. Before it reaches the high attenuation region, approximately the height at which the HAPS is stationed, it suffers low beam divergence. Due to low beam divergence, the FSO beam of the single-hop system will have similar geometry as that transmitted by HAPS. So, we see no gain in the system performances of the dual-hop system with respect to the single-hop system. While for the up-link scenario we see a diversity gain in the performance parameters of the dual-hop w.r.t. single-hop system. When the beam first travellers in high attenuation region it suffers high divergence. As it reaches the low attenuation region up to the height of HAPS, the beam divergence is high. For the single-hop system, this beam continues till LEO while the dual-hop system sends a new FSO signal from this height effectively eliminating the beam divergence. This leads to the better system performance of the dual-hop system for the up-link scenario. Similar trends will be seen throughout, so the following graphs plotted for the up-link scenario for both the single-hop and dual-hop systems.

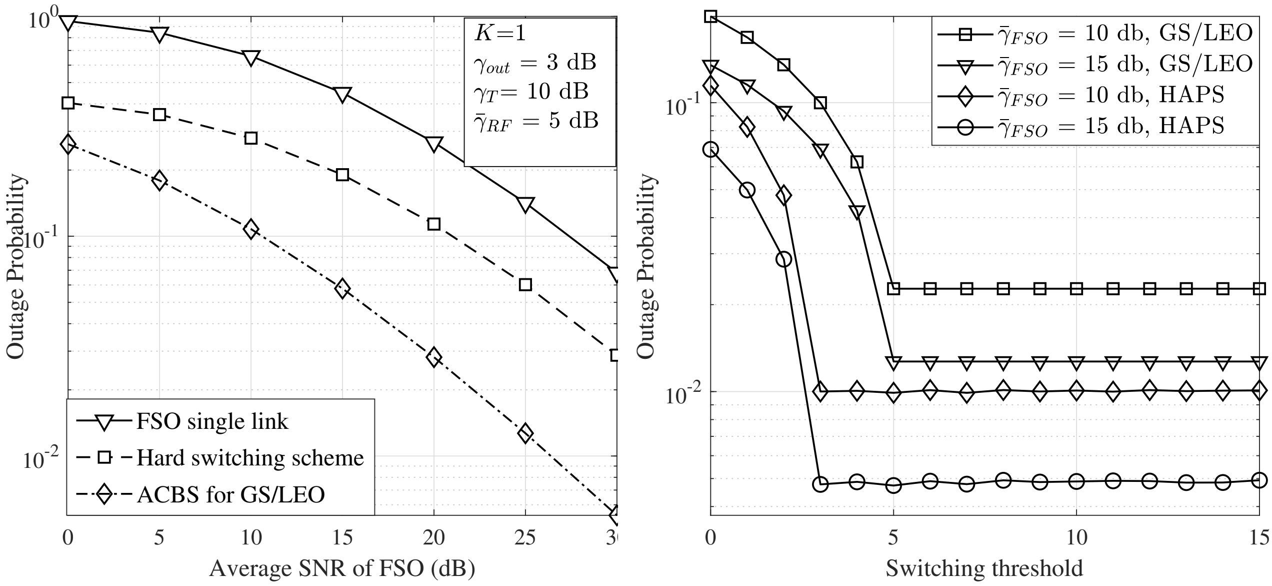

(a) Comparison with different switching schemes

(b) Optimum switching threshold

Figure 5.2: Comparison of ACBS with different switching schemes based on outage performance and outage probability vs γ_T for varying $\bar{\gamma}_{FSO}$

The figure (5.2a) shows the comparison of outage probability of different switching scheme for a single-hop up-link scenario. From the plots, we can observe that single ACBS hybrid FSO/RF performs better than the single link FSO system and hard-switching based hybrid FSO/RF system [15]. Here we can see that ACBS outperforms the single link FSO by 17.5 dB gain and the hard-switching-scheme [15] by 10 dB gain at outage probability of 10^{-1}.

The figure (5.2b) shows us the outage performance versus switching threshold with varying $\bar{\gamma}_{FSO}$ of single-hop and dual-hop hybrid FSO/RF systems. Note that GS/LEO represents the single-hop scenario, while HAPS represents the dual-hop scenario. For single-hop, the outage performance is plotted at $\gamma_{out} = 5$dB while for dual-hop it is plotted at $\gamma_{out} = 3$dB. From the figure, we can observe that as the switching threshold increase the outage probability of the system decreases and then it becomes constant. For $\gamma_T \geq \gamma out$ the outage probability of the system is constant. The value of γ_T for which the outage probability is minimum does not change even with varying $\bar{\gamma}_{FSO}$. So, we fix $\gamma_T \geq \gamma out$ for the optimum system performance.

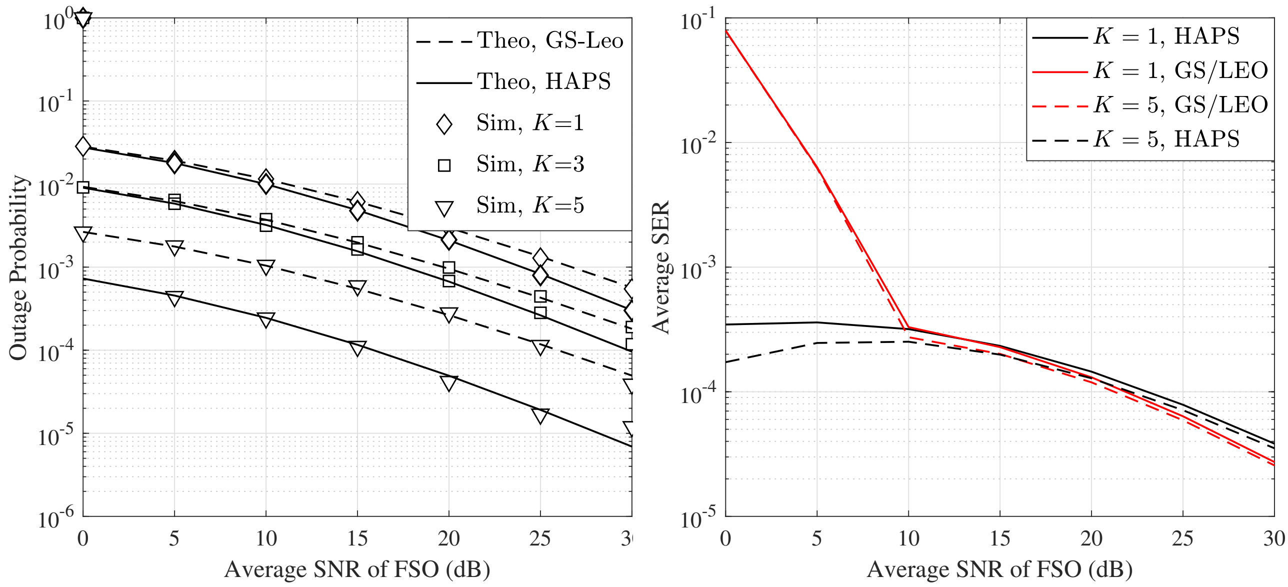

(a) Outage

(b) Average SER

Figure 5.3: System performance parameters vs $\bar{\gamma}_{FSO}$ for varying K

Figure (5.3a) shows the effect of Ricean factor on the outage probability of SH and DH hybrid FSO/RF system. From the plots, we can observe that with the increase in Ricean factor, the outage performance increases. We can achieve higher a coding gain from the outage performance of both the systems as K increases. As K decreases, we can observe a higher diversity gain in the outage performance of DH w.r.t. SH hybrid system.

Figure (5.3b) shows the effect of Ricean factor on the average SER of SH and DH hybrid FSO/RF system. Results are similar to the outage performance. From the plots, we can observe that with the increase in Ricean factor, the system performance increases. We can see a coding gain in the average SER performance of both the systems as K increases.

So we can infer from the figure (5.3) that as K increase the system performance increases. We get a coding gain in the plots of the system performance of SH and DH hybrid system. For the lower value of K, the DH system has higher diversity gain as compared to the higher value of K.

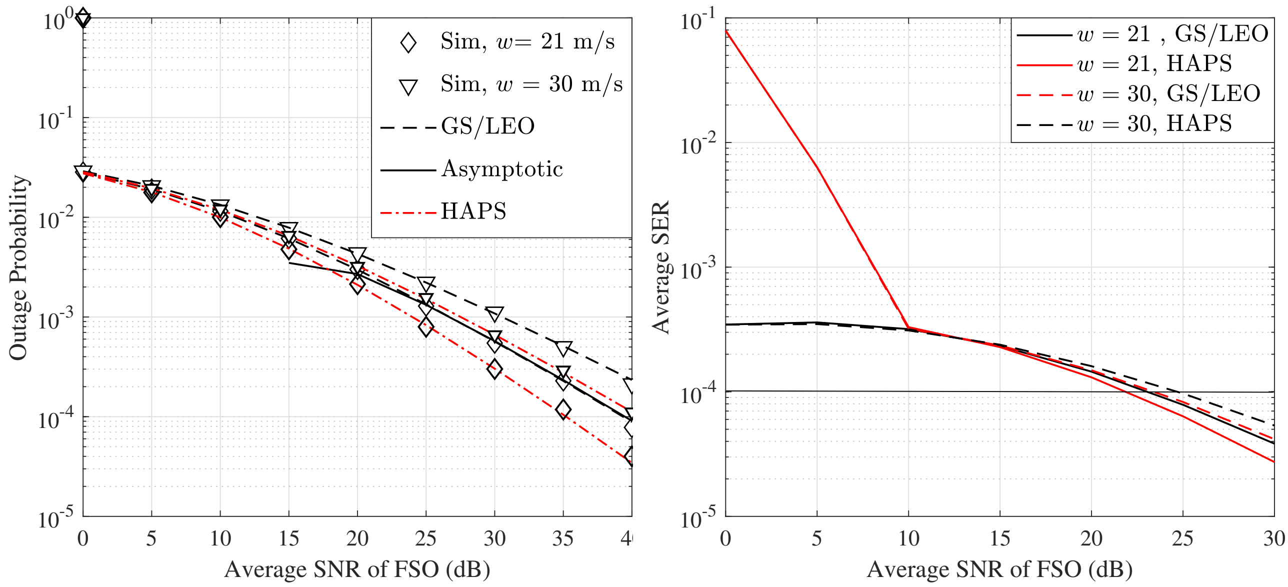

(a) Outage

(b) Average SER

Figure 5.4: System performance parameters vs $\bar{\gamma}_{FSO}$ for different wind speed

In figure (5.4), we see the variation of system performance parameters with varying wind speed. From figure (5.4a), we can observe that with the increase in wind speed the outage performance of the SH and DH hybrid systems deteriorates. We see diversity gain in SH and DH systems as wind speed increases. As wind speed increases, the formation of vortexes in air increases, effectively changing the refractive index of the medium, causing pointing errors and higher randomness in the received signal amplitude. This can cause degradation in system performance, which can be observed from the trends.

Similar trends are observed in the case of average SER of the DH and SH hybrid systems. From figure (5.4b), we can see that as wind speed increases the diversity order of the system decreases. And so the average SER performance of the systems deteriorates at higher.

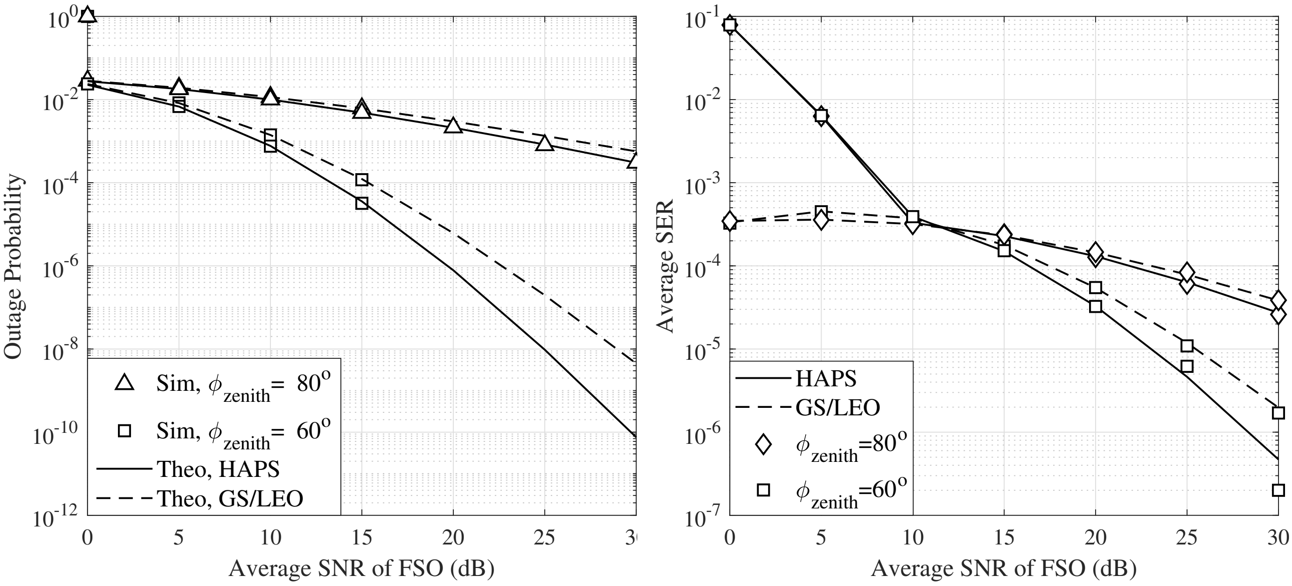

(a) Outage

(b) Average SER

Figure 5.5: System performance parameters vs $\bar{\gamma}_{FSO}$ for varying ϕ_{zenith}

In figure (5.5), we see the variation of system performance with varying zenith angle. With increases in the zenith angle, the propagation distance of the FSO beam increases. This increases the divergence of the FSO beam, thus degrading the system performance. This trend can be observed from the figure (5.5a) and (5.5b). As zenith angle increases the diversity order of the outage and average SNR of SH and DH hybrid system decreases.

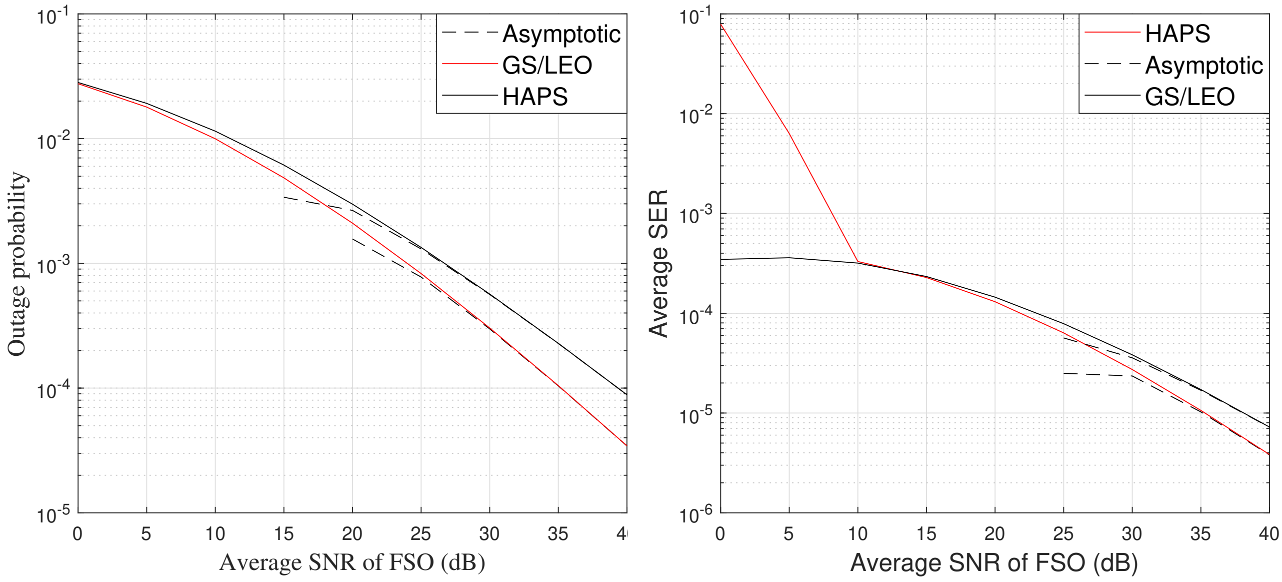

(a) Outage

(b) Average SER

Figure 5.6: Plots of asymptotic expressions and closed form expressions of system performance parameters vs $\bar{\gamma}_{FSO}$

Figure 5.6 shows the plots of asymptotic expressions and closed-form expressions of system performance parameters as can be observed from the figure the plots of asymptotic expressions trace the closed-form expressions at higher values of average SNR of the FSO link. The asymptotic expressions are faster to compute so are efficient to analyse the system performance parameters at higher values of SNR values. These are also efficient for computing the diversity order of the system.

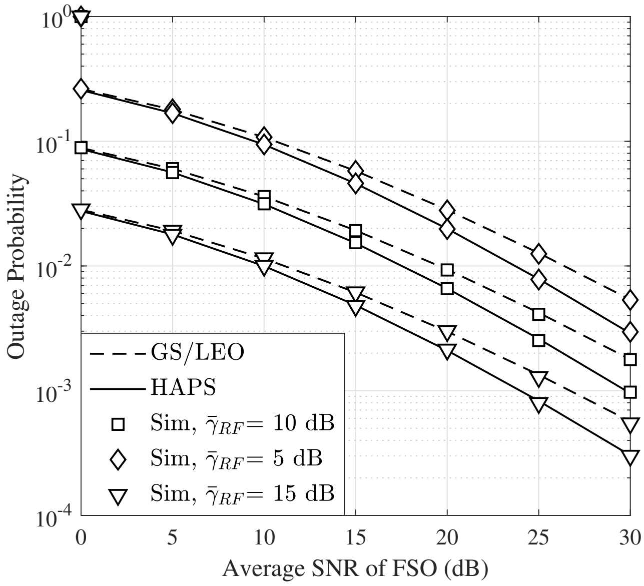

Figure 5.7: System performance parameters vs $\bar{\gamma}_{FSO}$ for up-link and down-link

The figure (5.7) shows the variation of outage probability with varying average SNR RF. The increase in the value of average SNR RF represents a better backup RF link. A better RF link directly translates to better system performance. This trend can be observed from the figure (5.7). As the value of average SNR RF increases the, we see a coding gain in the SH and DH systems.

Chapter 6

Conclusions and future works

Single link FSO systems have shown the potential to be the next step for the satellite communication system. FSO, while having its limitations, when backed by reliable RF, can be used in hybrid FSO/RF systems with novel switching scheme to draw out the full potential of the FSO. From figure (5.2a), we can say that adaptive combining based switching hybrid FSO/RF system performs better than the hard switching based hybrid FSO/RF system and single link FSO system. Building on this, we have extended the analysis of ACBS hybrid FSO/RF system to single-hop and dual-hop SATCOM for both the up-link and down-link scenario. Further, the closed-form expressions of the system performance parameters are derived. The performance of the SH and DH hybrid system are simulated assuming weak to strong atmospheric turbulence conditions for the FSO links and Ricean distribution for the RF links.

6.1 Conclusions

6.1.1 Single-hop hybrid FSO/RF system

- In sections (2.3.1) and (2.3.2) we have derived the closed-form expression for outage probability and average SER of single-hop adaptive combining based hybrid FSO/RF system respectively.

- We have determined the range of switching threshold for which the SH hybrid system gives the optimum switching threshold.

- In sections (4.1.1) and (4.2.1) the asymptotic analysis of system performance parameters of the single-hop hybrid system is carried out. The asymptotic expression provides a computationally faster way to analyse the diversity order and coding gain of the system.

- In chapter 5 we can see the variation of system performance parameters with different parameters plotted against average SNR of the FSO link. Form chapter 5, we can observe that as the FSO beam goes through higher atmospheric turbulence, examined by varying wind speed, the performance of the system deteriorates.

- With the increase in zenith angle, the propagation distance of the beam increases leaving it more vulnerable to the beam wander induced pointing error and atmospheric turbulence, which significantly affects the diversity order of the system.

- With the increase in the value of Ricean factor and average SNR of RF link, i.e. a better line of sight component and a better RF link respectively, the system performance of SH ACBS hybrid system improves.

6.1.2 Dual-hop hybrid FSO/RF system

- In sections (3.2.1) and (3.2.2) we have derived the closed-form expressions of system performance parameters. These expressions are verified using Monte Carlo simulations and are plotted in the chapter (5).

- In sections (4.1.2) and (4.2.2) the asymptotic expressions of the outage probability and average SER of DH ACBS hybrid FSO/RF system are discussed. Plots of the asymptotic expressions are shown in the chapter (5).

- We have derived an optimum switching threshold for best outage performance of the system.

- DH ACBS hybrid FSO/RF system performs better than the SH ACBS hybrid FSO/RF system in the case of the uplink scenario. While the system performance of DH and SH remains the same in the downlink scenario.

- The trend observed in the system performance parameters of DH hybrid system is similar to the SH hybrid system. With the increase in zenith angle or wind speed, the system performance of the system degrades. The higher value of Ricean factor and average SNR of the RF link result in better system performance.

6.2 Future works

In this thesis, we have only analysed outage probability and average SER of the ACBS hybrid FSO/RF system. This report discusses SISO hybrid FSO/RF system, assuming no shadowing for RF link.

There is a scope for a more detailed analysis of the system. Carrying out ergodic capacity analysis, extending the discussion to MIMO hybrid FSO/RF system and using a more generalised Malaga and $\alpha - \eta - \kappa - \mu$ distribution for channel modeling will be the future work direction.

Bibliography

[1] Dillow, Clay, Aug. 2013. Accessed on: Nov. 20 2019 [Archived]. Available on: https://www.webcitation.org/6Nx5VDQKZ?url=http://tech.fortune.cnn.com/2013/08/23/solara-rone/

[2] David Grace, Mihael Mohorcic, Introduction, *Broadband Communications Via High-Altitude Platforms 1*, Wiley Telecom, 2011.

[3] M. A. Khalighi and M. Uysal, "Survey on Free Space Optical Communication: A Communication Theory Perspective," *IEEE Communications Surveys & Tutorials*, vol. 16, no. 4, pp. 2231-2258, Fourth quarter 2014.

[4] V. W. S. Chan, "Optical satellite networks," in *Journal of Lightwave Technology*, vol. 21, no. 11, pp. 2811-2827, Nov. 2003.

[5] H. Kaushal and G. Kaddoum, "Optical communication in space: challenges and mitigation techniques," *IEEE Communications Surveys & Tutorials*, vol. 19, no. 1, pp. 57-96, First quarter, 2017. 169-205.

[6] Z. Sodnik, B. Furch and H. Lutz, "Free-Space Laser Communication Activities in Europe: SILEX and beyond," in *procc IEEE Lasers and Electro-Optics Society*, Montreal, Que., 2006, pp. 78-79.

[7] T. Jono, Y. Takayama, K. Shiratama, I. Mase, B. Demelenne, Z. Sodnik, A. Bird, M. Toyoshima, H. Kunimori, D. Giggenbach, N. Perlot, M. Knapek, K. Arai, "Overview of the inter-orbit and the orbit-to-ground laser communication demonstration by OICETS", SPIE, vol. 6457, pp. 645702-1-645702-10, 2007

[8] H. Hemmati, A. Biswas and I. B. Djordjevic, "Deep-space optical communications: Future perspectives and applications," in*Proc. of the IEEE*, vol. 99, no. 11, pp. 2020-2039, Nov. 2011.

[9] A. Viswanath, P. Gopal, V. K. Jain and S. Kar, "Performance enhancement by aperture averaging in terrestrial and satellite free space optical links," in *IET Optoelectronics*, vol. 10, no. 3, pp. 111-117, 6, 2016.

[10] Minh Q. Vu, Nga T.T. Nguyen, Hien T.T. Pham, Ngoc T. Dang, "Performance enhancement of LEO-to-ground FSO systems using All-optical HAP-based relaying," *Physical Communication*, vol. 31, pp. 218-229, 2018

[11] F. Fidler, M. Knapek, J. Horwath and W. R. Leeb, "Optical Communications for High-Altitude Platforms," in *IEEE Journal of Selected Topics in Quantum Electronics*, vol. 16, no. 5, pp. 1158-1070, Sept.-Oct. 2010.

[12] M. Q. Vu, N. T. T. Nguyen, M. B. Vu, H. T. T. Phan, H. T. T. Pham and N. T. Dang, "HAP-based FSO system using all-optical detect-amplify-and-forward relaying and coherent detection receiver," *NAFOSTED Conference on Information and Computer Science*, Hanoi, 2017, pp. 120-125.

[13] N. D. Chatzidiamantis, G. K. Karagiannidis, E. E. Kriezis and M. Matthaiou, "Diversity Combining in Hybrid RF/FSO Systems with PSK Modulation," in *Proc. 2011 IEEE International Conference on Communications (ICC)*, Kyoto, pp. 1-6, 2011.

[14] M. Usman, H.-C. Yang and M.-S. Alouini, "Practical switching-based hybrid FSO/RF transmission and its performance analysis," *IEEE J.Photon.*, vol. 6, no. 5, pp. 1–13, Oct. 2014.

[15] S. Sharma, A. S. Madhukumar and R. Swaminathan, "Switching-based cooperative decode-and-forward relaying for hybrid FSO/RF networks," *IEEE J. Opt. Commun. Netw.*, vol. 11, no. 6, pp. 267-281, June 2019.

[16] T. Rakia, H. Yang, M. Alouini and F. Gebali, "Outage Analysis of Practical FSO/RF Hybrid System With Adaptive Combining," *IEEE Communications Letters*, vol. 19, no. 8, pp. 1366-1369, Aug. 2015.

[17] H. Kaushal, V. K. Jain, S. Kar, in *Free Space Optical Communication*, Springer India, 2017.

[18] M. K. Simon and M.-S. Alouini, *Digital Communications Over Fading Channels: A Unified Approach to Performance Analysis*, 2nd ed. New York, NY, USA: Wiley-Interscience, 2005.

[19] V. S. Adamchik, and O. I. Marichev, "The algorithm for calculating integrals of hypergeometric type functions and its realization in REDUCE system," in *Proc. Int. Symp. Symbolic and Algebraic Computation*, pp. 212–224, Tokyo, Japan, 1990.

[20] A. Viswanath, V. K. Jain and S. Kar, "Analysis of earth-to-satellite free-space optical link performance in the presence of turbulence, beam-wander induced pointing error and weather conditions for different intensity modulation schemes," in *IET Communications*, vol. 9, no. 18, pp. 2253-2258, 17 12 2015.

[21] I. Wolfram Research, *Mathematica Edition: Version 8.0. Champaign*, Illinois: Wolfram Research, Inc., 2010.

Publications

1. Siddharth Mokkapati, Suyash Shah, and Swaminathan R., "Outage Analysis of Adaptive Combining Scheme for Hybrid FSO/RF Communication," submitted to *IEEE National Conference on Communications (NCC)*, Kharagpur, India, 2020.

2. Suyash Shah, Siddharth Mokkapati, and Swaminathan R, "Performance analysis of SAGIN with hybrid optical/RF communication," to be submitted to *IEEE journals/ transactions*.

3. Siddharth Mokkapati, Suyash Shah, and Swaminathan R, "Performance analysis of adaptive combining based hybrid FSO/RF terrestrial communication," to be submitted to *IEEE journals/ transactions*.